

# Accepted Manuscript

Structure-based design, synthesis, and biological evaluation of withaferin A-analogues as potent apoptotic inducers

Gabriel G. Llanos, Liliana M. Araujo, Ignacio A. Jiménez, Laila M. Moujir, Jaime Rodríguez, Carlos Jiménez, Isabel L. Bazzocchi



PII: S0223-5234(17)30686-4

DOI: [10.1016/j.ejmech.2017.09.004](https://doi.org/10.1016/j.ejmech.2017.09.004)

Reference: EJMECH 9719

To appear in: *European Journal of Medicinal Chemistry*

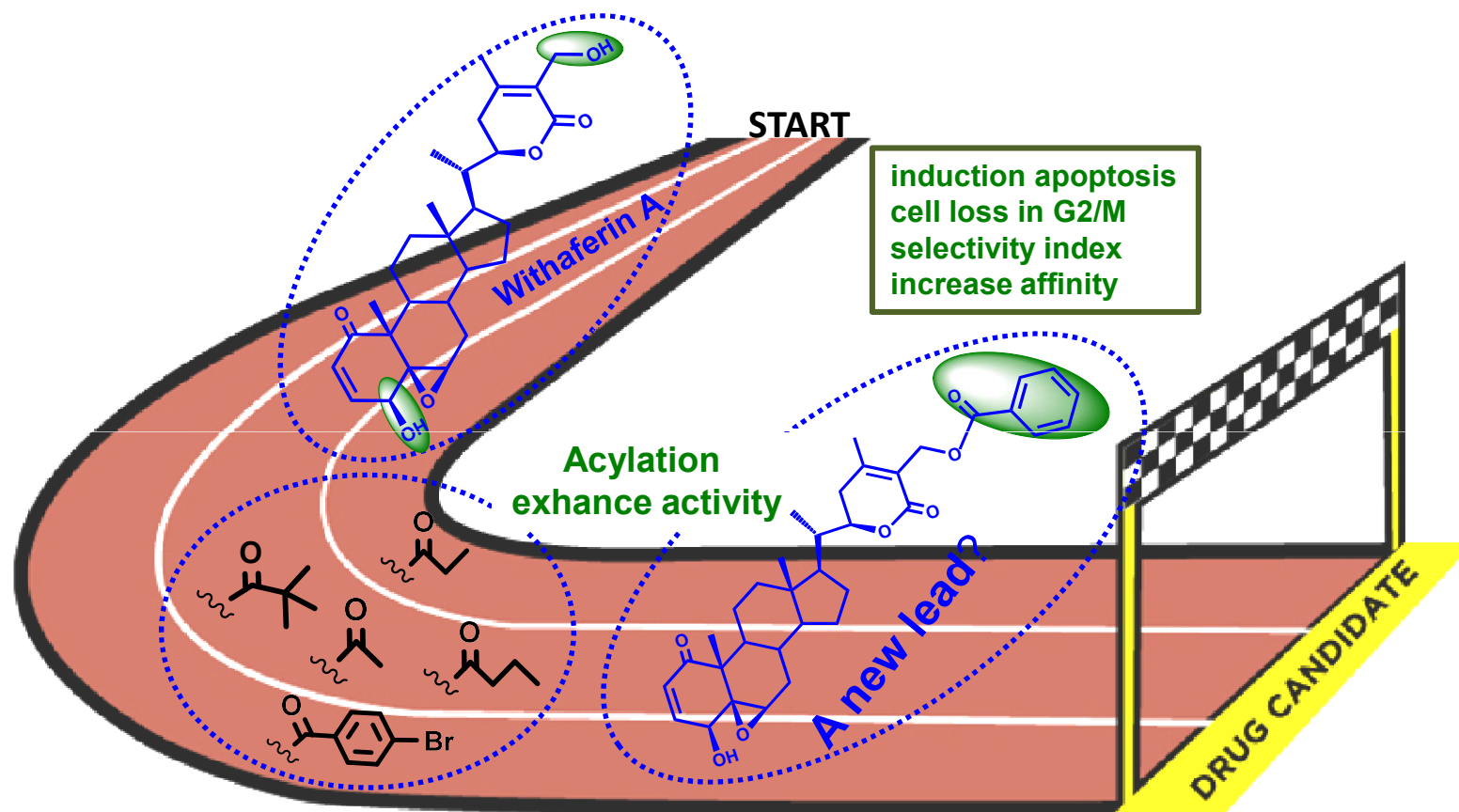
Received Date: 26 April 2017

Revised Date: 1 September 2017

Accepted Date: 3 September 2017

Please cite this article as: G.G. Llanos, L.M. Araujo, I.A. Jiménez, L.M. Moujir, J. Rodríguez, C. Jiménez, I.L. Bazzocchi, Structure-based design, synthesis, and biological evaluation of withaferin A-analogues as potent apoptotic inducers, *European Journal of Medicinal Chemistry* (2017), doi: 10.1016/j.ejmech.2017.09.004.

This is a PDF file of an unedited manuscript that has been accepted for publication. As a service to our customers we are providing this early version of the manuscript. The manuscript will undergo copyediting, typesetting, and review of the resulting proof before it is published in its final form. Please note that during the production process errors may be discovered which could affect the content, and all legal disclaimers that apply to the journal pertain.



**Withaferin A Optimization as Apoptotic Inducer**

# Structure-based design, synthesis, and biological evaluation of Withaferin A-analogues as potent apoptotic inducers

Gabriel G. Llanos <sup>a</sup>, Liliana M. Araujo <sup>b</sup>, Ignacio A. Jiménez <sup>a</sup>, Laila M. Moujir <sup>b</sup>, Jaime Rodríguez <sup>c</sup>, Carlos Jiménez <sup>c</sup>, and Isabel L. Bazzocchi <sup>a,\*</sup>

<sup>a</sup> *Instituto Universitario de Bio-Orgánica Antonio González, Departamento de Química Orgánica, and Instituto Canario de Investigación del Cáncer, Universidad de La Laguna, Avenida Astrofísico Francisco Sánchez 2, 38206 La Laguna, Tenerife, Spain*

<sup>b</sup> *Departamento de Bioquímica, Microbiología, Genética y Biología Celular, Universidad de La Laguna, Avenida Astrofísico Francisco Sánchez s/n, 38206 La Laguna, Tenerife, Spain*

<sup>c</sup> *Departamento de Química Fundamental, Facultad de Ciencias e Centro de Investigaciones Científicas Avanzadas (CICA), Universidad da Coruña, 15071 A Coruña, Spain*

\* Corresponding author. Tel.: +34 922 318594; fax: +34 922 318571. *E-mail address:* ilopez@ull.es (I.L. Bazzocchi).

**Abstract:** Apoptosis inducers represent an attractive approach for the discovery and development of anticancer agents. Herein, we report on the development by molecular fine tuning of a withaferin A-based library of 63 compounds (**2-64**), 53 of them reported for the first time. Their antiproliferative evaluation on HeLa, A-549 and MCF-7 human tumor cell lines identified fifteen analogues displaying higher activity ( $IC_{50}$  values ranging 0.3-4.8  $\mu$ M) than the lead ( $IC_{50}$  values ranging 1.3-10.1  $\mu$ M) either in lag or log growth phases. SAR analysis revealed that acylation enhances cytotoxicity, suggesting the hydrophobic moiety contributes to the activity, presumably by increasing affinity and/or cell membrane permeability. Further investigation clearly indicated that compounds **3**, **11**, **12**, and **18** induce apoptosis evidenced by chromatin condensation, phosphatidylserine externalization, and caspase-3 activation effects on HeLa cells. The potent capacity to induce apoptosis with concomitant cell loss in G2/M highlights the potential of 27-benzyl analogue (**18**) as an apoptotic inducer drug candidate.

**Keywords:** Withaferin A; Compound library; Cytotoxicity; Apoptosis; Structure-activity relationship.

## 1. Introduction

Cancer has become the second largest cause of death in many countries [1]. Inhibition of apoptotic pathways is recognized as an important hallmark for cancer, since blocking apoptosis could lead to excessive cell proliferation as well as resistance to cancer treatments [2]. Therefore, the identification of apoptosis inducers represents an attractive approach for the discovery and development of potential anticancer agents.

Withanolides are structurally diverse steroidal compounds with an ergosterol skeleton in which C-22 or C-23 and C-26 are oxidized to form a  $\delta$ - or  $\gamma$ -lactone ring on the nine-carbon side chain [3]. These compounds have attracted considerable attention due to their potential in drug research and development [4]. Withaferin A (WA) is one of the main biologically active withanolides, exerting a wide range of biological properties [5]. WA has been shown to suppress cell proliferation either in a variety of cancer cells in culture and in mouse xenograft tumor models [6]. Mechanisms underlying anticancer effects of WA appear to vary and hence may be cell-type specific, involving multiple key cell-survival and regulatory pathways [7]. Molecular events associated with WA-induced apoptosis include, G2/M phase cell cycle arrest [8], enhancement of reactive oxygen species (ROS) production [9], activation of caspases and inhibition of NF- $\kappa$ B pathway [10], stabilization of p53 family members [11], induction of endoplasmic reticulum (ER) stress [12], Gas6/Axl-mediated down-regulation of the STAT3 signalling pathway [13], FOXO3a-dependent apoptosis [14], regulation of the expression of death receptor 5 (DR5) [15], down-regulation of anti-apoptotic proteins Bcl-2 and Mcl-1 [16], and disruption of the vimentin cytoskeleton [17].

Despite a great deal of research conducted on the potential anticancer properties of WA, there are few reports available on its structural modifications. In fact, a small library of 2,3-dihydro, 3 $\beta$ -substituted WA derivatives have been synthesized through regio-/stereoselective Michael addition to ring A, and the 3-azido analogue increased in

cytotoxicity against various cancer cell lines [18]. To identify features responsible for the divergent biological activities ascribed to WA, Gunatilaka *et al.* examined a series of natural, and chemical and microbial transformed WA related products as inducers of the cellular heat-shock response [19] and as chaperone p97 inhibitors [20]. Mondal *et al.* described ten novel *spiro*-pyrrolizidine-oxindole adducts of WA, achieving via an intermolecular 1,3-dipolar azomethine-ylide cycloaddition, and their evaluation led to four promising anticancer compounds [21]. Recently, two structurally simplified WA analogues have been reported [22]. Therefore, not only studies on the elucidation of the mechanism of anticancer activity of WA, but also on the synthetic exploitation of its scaffold and the discovery of new leads will continue to be a challenging field of research.

In the search for new suitable anticancer agents, we previously reported two WA-derivatives as potent apoptosis inducers in cancer cells [23,24]. To shed light on the structural requirements for WA steroid-framework activity, and to provide new lead compounds with improved therapeutic potential, the present study reports the design, synthesis, anti-proliferative effects, and SAR analysis of a WA-based library consisting of 63 analogues. Selected analogues were further investigated for their ability to induce apoptosis.

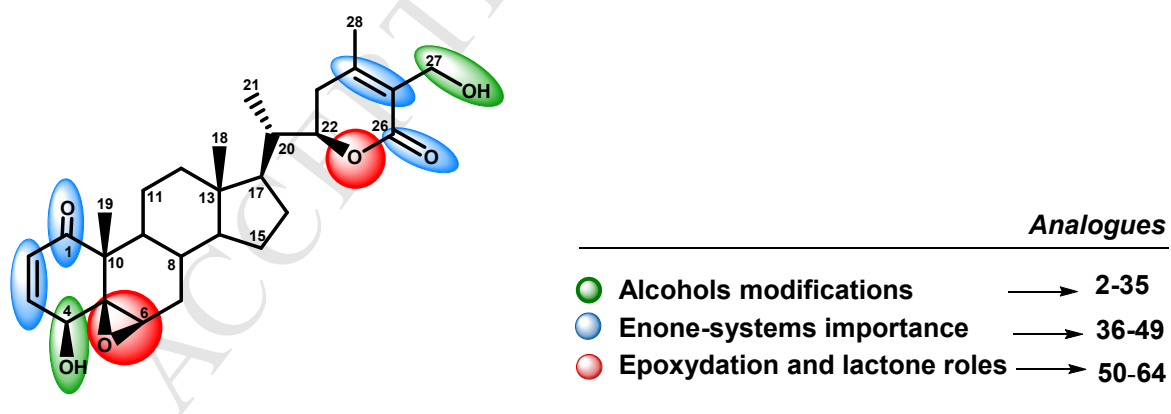
## 2. Results and discussion

### 2.1. Chemistry

In an attempt to enhance anticancer activity and having a better knowledge of the structure-activity relationships of WA-framework, a library of 63 withaferin A-analogues (**2-64**) were designed and synthesized. WA (**1**) appeared to be readily available by extraction from the leaves of *Withania aristata* [24], with more than a 4.5% yield from the CH<sub>2</sub>Cl<sub>2</sub>

extract, as well as being a well known anticancer prototype lead [7], make it suitable as a starting material.

Chemical structure analysis of WA suggests three suitable positions on its steroid-backbone to nucleophilic attack which could be involved in covalent binding at cysteine residues in target protein [8,25]. These include: (i) the  $\alpha,\beta$ -unsaturated ketone group in ring A, (ii) the  $5\beta,6\beta$ -epoxide in ring B, and (iii) the  $\alpha,\beta$ -unsaturated 6-membered lactone in ring E. Thus, based on the WA-framework, a series of analogues (**2-64**), divided in three groups (Fig. 1), were prepared by standard methods as described in Schemes 1-6 and detailed in the Supporting Information (S56-S82). Therefore, the first step in this task was to investigate the role of hydroxyl groups at C-4 and C-27 by converting them into ester, ether, ketone, aldehyde or halo derivatives (analogues **2-35**). Secondly, modification on the enone-system was carried out by interchanging the alkene into alkane, epoxide, amine or ether functionalities as well as the carbonyl into alcohol functionality (analogues **36-49**). Finally, opening of the epoxy group to give alcohol, diol, alkane or halohydrin groups yielded different heterocyclic compounds (analogues **50-64**).

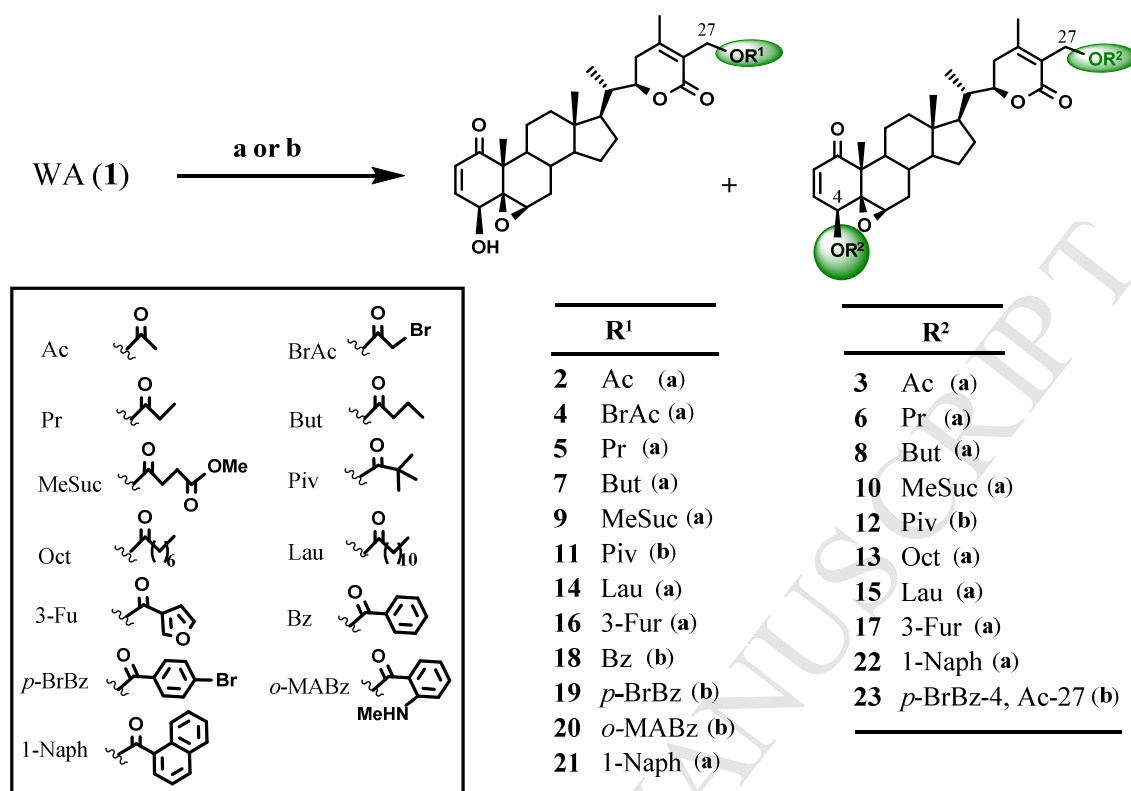


**Fig. 1.** Plausible structural features modifications for withaferin A.

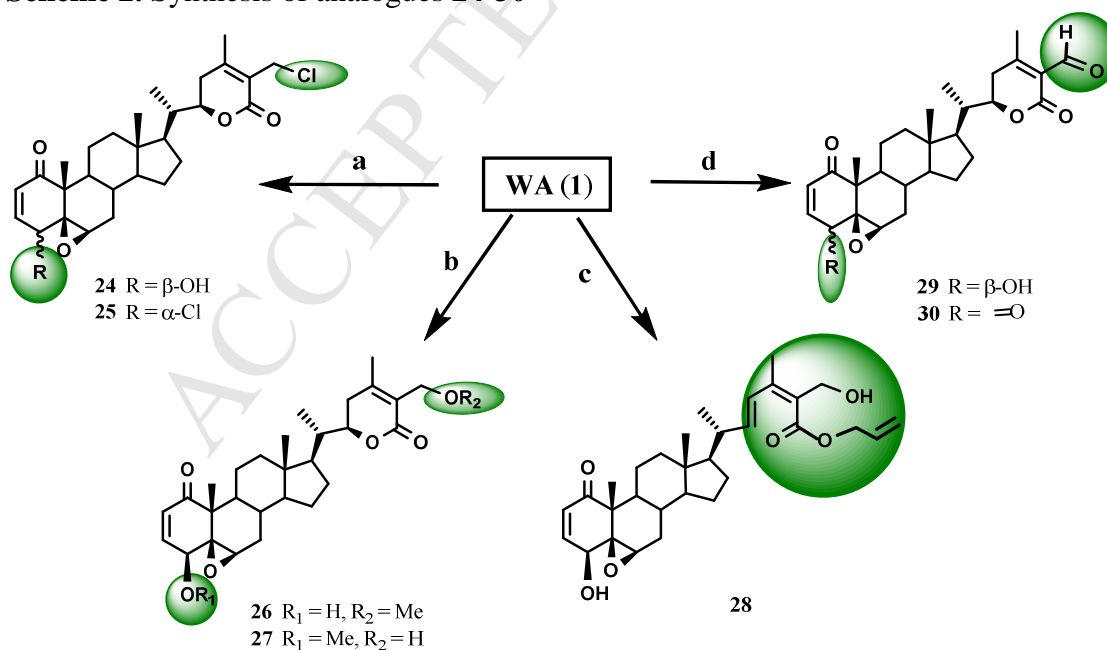
### 2.2.1. Modifications of the hydroxyl groups

To explore the role of the hydroxyl groups on cytotoxic activity, compounds **2-23** were prepared by acylation of **1** with alkyl anhydrides, and alkyl or aryl acid chlorides of different sizes, lipophilicity and stereoelectronic properties. Thus, 27-monoester and 4,27-diester derivatives were synthesized following the strategy outlined in Scheme 1 (S56-S65 in SI). Due to the dissimilar reactivity of acylating reagents and hydroxyl groups in the starting material, different reaction conditions were performed. The following series of analogues (**24-30**) have also been prepared to explore more thoroughly the relevance of the hydroxyl groups on the cytotoxic activity (Scheme 2, S65-S68 in SI). Therefore, the chlorinated steroids **24** and **25** were obtained by chlorination of **1** with thionyl chloride in dichloromethane. The *O*-4 or *O*-27-methyl analogues (**26** and **27**) were synthesized by treatment of WA with methyl iodide and sodium hydride in tetrahydrofuran. Subsequently, *O*-alkylation of **1** with allyl bromide by using similar reaction conditions as before yielded **28** instead of the expected *O*-allylic analogue. Opening, dehydrogenation and dienone formation of the lactone ring present in **1** could explain the formation of analogue **28**. Moreover, oxidation of **1** with Jones reagent at 0 °C yielded analogues **29** and **30** bearing the expected aldehyde at C-27 and the  $\beta$ -hydroxyl or keto group at C-4, respectively.

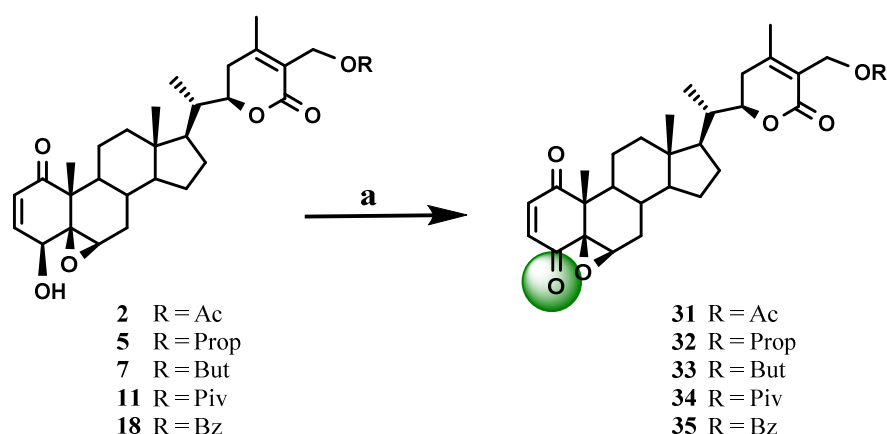
Previously reported structure-activity relationship (SAR) studies on withanolides [24], indicated that compounds bearing a ketone at C-4 have a selective pharmacological profile. Encouraged by these results, derivatives **31-35** were prepared from compounds **2**, **5**, **7**, **11**, and **18**, respectively, by treatment of with chromium trioxide in pyridine and dichloromethane (Scheme 3, S68-S70 in SI).

Scheme 1. Synthesis of acyl WA analogues 2-23<sup>a</sup>

<sup>a</sup> Reagents and conditions: (a) corresponding anhydride or acid chloride/halide, Et<sub>3</sub>N, CH<sub>2</sub>Cl<sub>2</sub>, 0 °C; (b) corresponding acid chloride or anhydride, Et<sub>3</sub>N, DMAP, CH<sub>2</sub>Cl<sub>2</sub>, r.t.

Scheme 2. Synthesis of analogues 24-30<sup>a</sup>

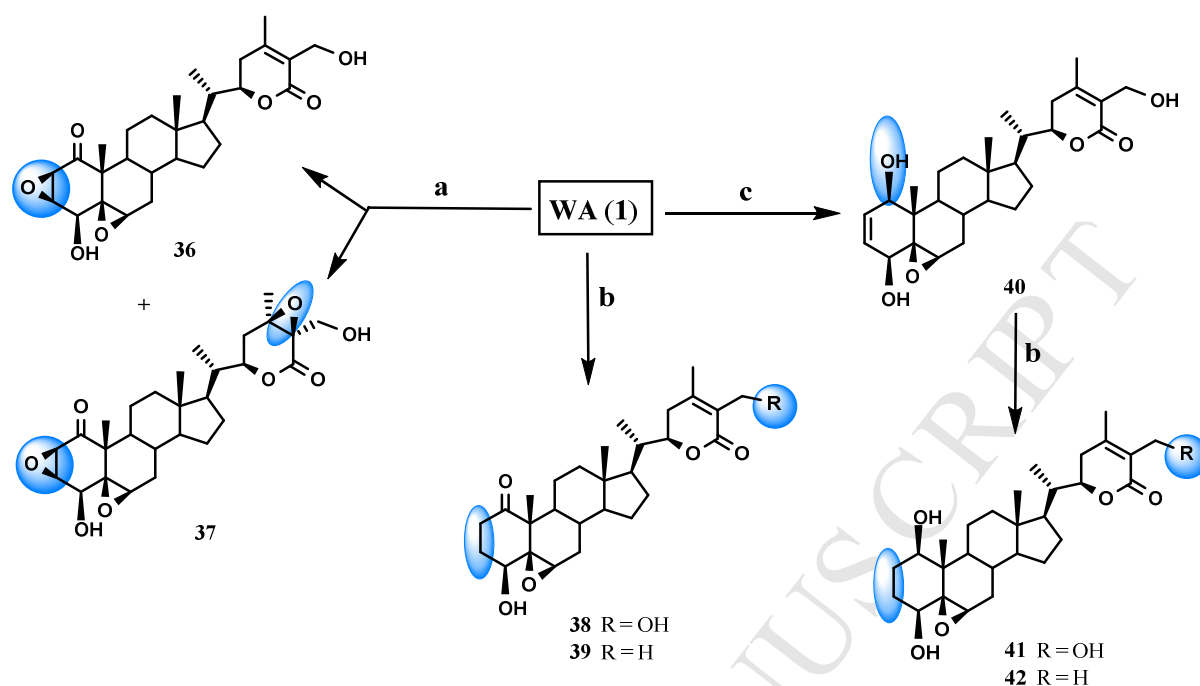
<sup>a</sup> Reagents and conditions: (a) Cl<sub>2</sub>SO, CH<sub>2</sub>Cl<sub>2</sub>, 0 °C → r.t.; (b) (1) NaH, THF, 0 °C (2) CH<sub>3</sub>I, 60 °C; (c) (1) NaH, THF, 0 °C → r.t. (2) allyl bromide, 60 °C; (d) CrO<sub>3</sub>/H<sub>2</sub>SO<sub>4</sub>, acetone, 0 °C.

**Scheme 3.** Synthesis of 4-oxo-WA analogues **31-35**<sup>a</sup>

<sup>a</sup> Reagents and conditions: (a) CrO<sub>3</sub>, py, CH<sub>2</sub>Cl<sub>2</sub>, 0 °C → r.t.

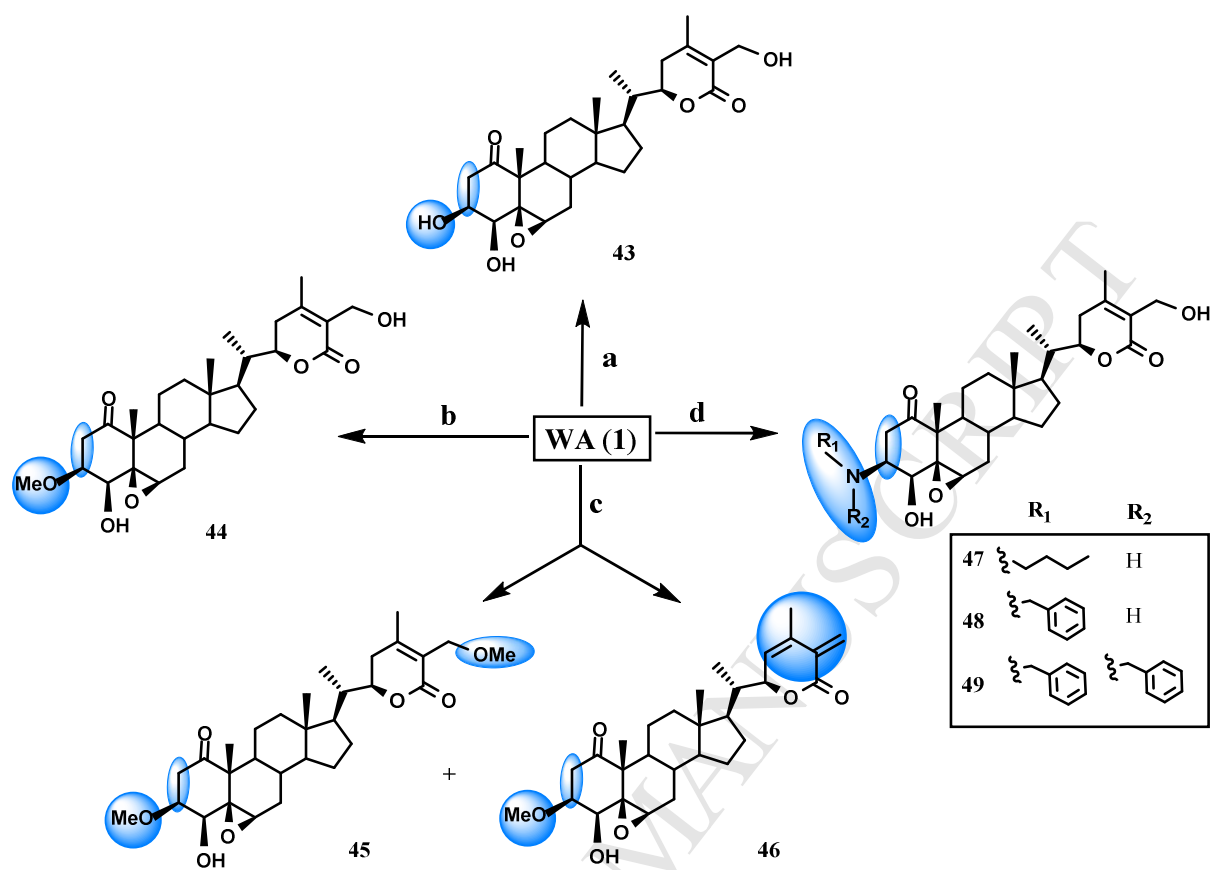
### 2.1.2. Modifications of the enone-systems

Taking into account the important role of the epoxy group on the cytotoxic activity of this type of natural compounds [21], analogues with an additional epoxy group between C2/C3 (**36**) or C24/C25 (**37**) were prepared by treatment of **1** with hydrogen peroxide and sodium hydroxide. The previous reports on the relevance of the 2-en-1-one motif for cytotoxicity was confirmed by selective reductions performed on **1** [18]. Thus, selective reduction of the double bond of the  $\alpha,\beta$ -unsaturated ketone with a catalytic amount of palladium hydroxide yielded derivatives **38** and **39**. Selective reduction of the keto group at C-1 was achieved following the Luche's procedure [26] by using sodium borohydride and cerium (III) chloride heptahydrate in methanol to give enol **40**, and subsequent reduction with hydrogen in presence of a catalytic amount of palladium hydroxide yielded derivatives **41** and **42** (Scheme 4, S70-S73 in SI).

**Scheme 4.** Synthesis of WA analogues **36-42**<sup>a</sup>

<sup>a</sup> Reagents and conditions: (a) H<sub>2</sub>O<sub>2</sub>, NaOH 4N, CH<sub>2</sub>Cl<sub>2</sub>/MeOH (1/2), r.t.; (b) H<sub>2</sub>, Pd(OH)<sub>2</sub>/C, MeOH, 4 bar, r.t.; (c) CeCl<sub>3</sub>·7H<sub>2</sub>O, NaBH<sub>4</sub>, MeOH, 0 °C.

To examine the influence of the  $\Delta^2$  double bond, the selective nucleophilic addition to the  $\alpha,\beta$ -conjugated carbonyl moiety was performed. The designed molecules **43**, **44** and **47-49** were synthesized via conjugated nucleophilic addition using different nucleophiles such as sodium hydroxide, sodium methoxide, *n*-butylamine, benzylamine, and dibenzylamine, according to Scheme 5. Due to the dissimilar reactivity of reagents, different reaction conditions were performed (S73-S75 in SI). Thus, treatment of **1** with 1.5 equivalents of sodium methoxide gave compounds **45** and **46**, whereas using 5 equiv. yielded compound **44**.

**Scheme 5.** Synthesis of 2,3-dihydro-WA analogues **43-49**<sup>a</sup>

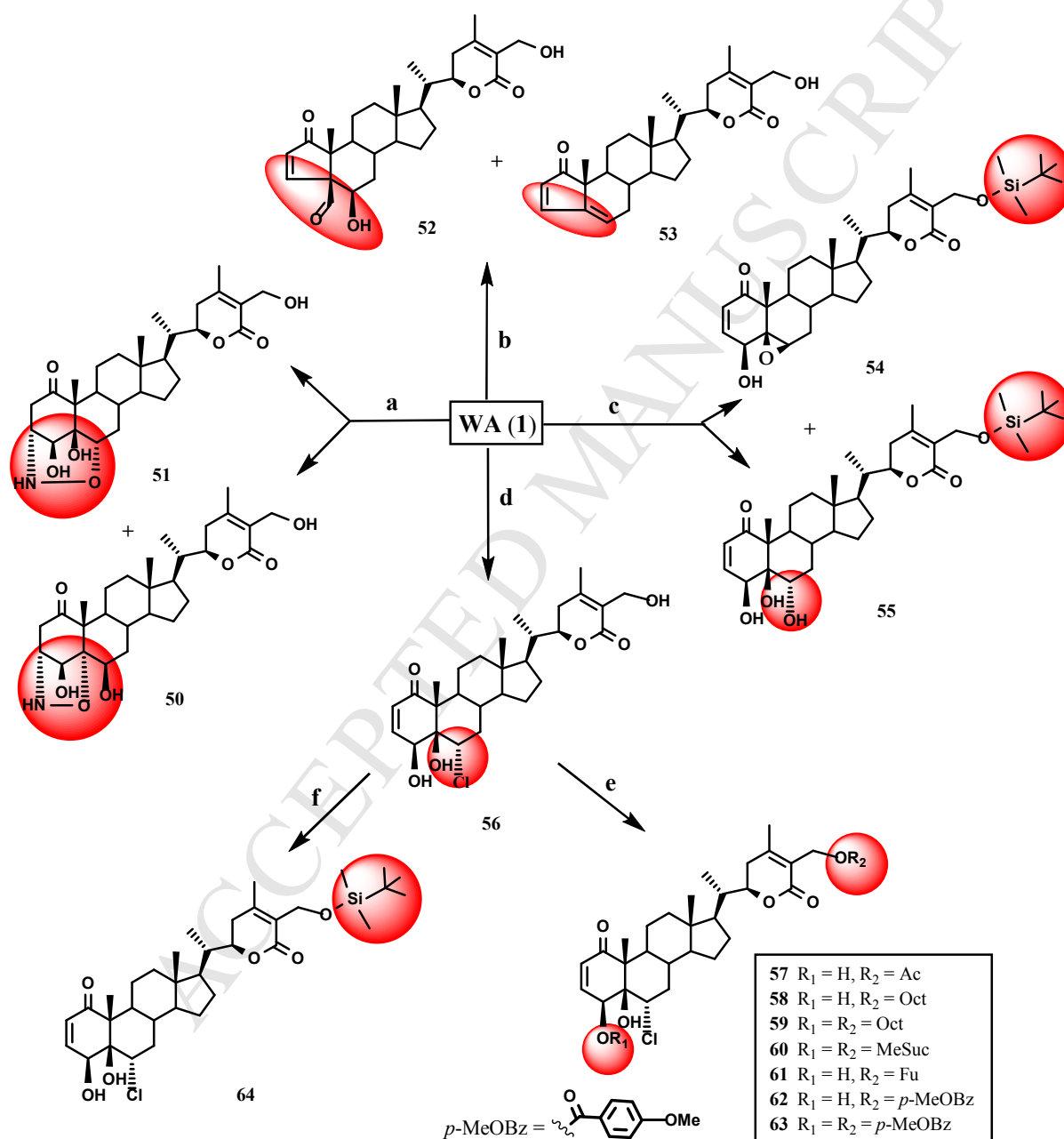
<sup>a</sup> Reagents and conditions: (a) NaOH, THF/H<sub>2</sub>O (1/1), 0 °C → r.t.; (b) NaOMe (1.5 equiv., 45 min), r.t.; (c) NaOMe (5 equiv., 48 h), r.t.; (d) Al<sub>2</sub>O<sub>3</sub>, *n*-butylamine, benzylamine or dibenzylamine, CH<sub>2</sub>Cl<sub>2</sub>, Ar, r.t.

### 2.1.3. Modifications to the 5 $\beta$ ,6 $\beta$ -epoxy group

The role of the 5 $\beta$ ,6 $\beta$ -epoxy group on activity was also analyzed. For this purpose, ring-opening reactions were carried out leading to analogues **50-55** (Scheme 6, S75-S77 in SI). The synthesis of compounds **50** and **51** with 5- and 6-member heterocyclic rings (S44-S45 in SI), respectively, involving epoxide-ring opening followed by Michael addition, was achieved by stirring **1** with hydroxylamine hydrochloride in pyridine. Compounds **52** and **53**, bearing a contracted A-ring [27], were prepared by treatment of **1** with boron trifluoride etherate in tetrahydrofuran. Earlier reports on the effect of silyl substituents on cancer cell proliferation [24] prompted us to prepare analogues **54**, **55** and **64**. Chloroesters **57-63** were synthesized from **1**, in two steps. First, WA was converted to the corresponding chlorohydrin

**56** by regioselective epoxide-ring opening with cerium (III) chloride heptahydrate in acetonitrile and tetrahydrofuran under reflux. Subsequent esterification of **56** with several carboxylic acid derivatives in dichloromethane afforded 6-chloroesters **57-63** (Scheme 6, S77-S82 in SI).

**Scheme 6.** Synthesis of 5,6-ring opening analogues (**50-55**) and **56** analogues (**57-64**)<sup>a</sup>



<sup>a</sup> Reagents and conditions: (a)  $\text{OHNH}_2 \cdot \text{HCl}$ , py, r.t.; (b)  $\text{BF}_3 \cdot \text{OEt}_2$ , THF,  $0^\circ\text{C} \rightarrow \text{r.t.}$ ; (c)  $\text{TBDMSCl}$ , imidazole, DMAP,  $\text{CH}_2\text{Cl}_2$ , r.t.; (d)  $\text{CeCl}_3 \cdot 7\text{H}_2\text{O}$ ,  $\text{CH}_3\text{CN}/\text{THF}$  (2/1), r.t.  $\rightarrow 85^\circ\text{C}$ ; (e)  $\text{Et}_3\text{N}$ ,  $\text{CH}_2\text{Cl}_2$ ,  $\text{Ac}_2\text{O}$ , octanoyl chloride, methyl succinyl chloride, 3-furoyl chloride or *p*-bromobenzoyl chloride,  $0^\circ\text{C}$ ; (f)  $\text{TBDMSCl}$ , DMAP, imidazole,  $\text{Cl}_2\text{CH}_2$ , r.t.

Among the former synthetic analogues, 54 out of 63 are reported for the first time. The structures of the new compounds were elucidated by HRMS and NMR data (S2-S55 in SI), whereas those of the previous reported analogues, compounds **2** [24], **3** [19,28], **30** [20], **31** [19], **38** [19], **43** [29], **44** [30], **52** [24], **54** [24] and **56** [31], were elucidated by comparison of their spectral data with those reported in the literature.

## 2.2. Biological Evaluation

### 2.2.1. Antiproliferative activity

In an attempt to identify more potent withanolides than the parent withaferin A (WA, **1**), the 50% *in vitro* antiproliferative concentrations of analogues **3-14**, **16-51**, **55**, and **57-64** were evaluated in three human cancer cell lines (cervix carcinoma HeLa, lung carcinoma A-549, and breast carcinoma MCF-7) and the Vero (African green monkey kidney) non-tumoral cell line, the latter used to test for selectivity. Compounds **15** and **53** were not assayed due to insolubility and limited amount available, respectively. The structure-activity study was expanded by the known cytotoxic activity of WA and compounds **2**, **52**, **54**, and **56**, previously reported by our group [23,24]. The results (Tables S83-S86 in SI) show that 41 of the studied compounds (66%) exhibited cytotoxic activity ( $IC_{50} \leq 20 \mu M$ ) toward at least two of the cancer cell lines. Among them, 31 analogues (50%) exhibited  $IC_{50}$  values ranging from 0.2-9.6  $\mu M$  in all tumor cells, either in lag or log growth phase (Table 1), and 15 derivatives (23.8%, compounds **3-8**, **11**, **12**, **16**, **18**, **20**, **23**, **24**, **34** and **54**) showed a higher cytotoxic activity ( $IC_{50}$  ranging 0.3-4.8  $\mu M$ ), than the reference compound WA ( $IC_{50}$  ranging 1.3-10.1  $\mu M$ ). At an individual level, the MCF-7 cell line was the most sensitive to analogues. In fact, 28 derivatives (44.4%) exhibited higher activity in at least one of the growth phases than WA and mercaptopurine, used as positive controls. Among these, derivatives **3**, **11**, **18**, and **23**

showed the most potent activity with  $IC_{50}$  values between 0.3  $\mu$ M and 0.8  $\mu$ M (Table 1). Similarly, HeLa cells underwent growth inhibition when exposed to derivatives **3**, **9**, **11**, **12**, **18**, and **54**, whereas in human A-549 cells only compounds **3** and **18** led to  $IC_{50}$  values  $\leq$  1  $\mu$ M. Of note, compounds **3**, **5**, **7**, **8**, **11**, **18**, and **23** (11.3%) displayed a significant cytotoxic activity ( $IC_{50} \leq 2.8 \mu$ M) in all tumor cell lines, whereby the ester derivatives **3** and **18** exerted the most remarkable inhibitory effect on cell growth.

Overall, the antiproliferative activity did not depend on the growth phase of the cells, demonstrated by the  $IC_{50}$  values of the compounds added either prior to or 24 h after cell seeding, i.e. during lag or exponential growth, respectively (Tables S83-S86 in SI). However, the  $IC_{50}$  values were more than three times lower in MCF-7 cells when adding analogues **16**, **33**, and **35** during exponential growth phase, comparable to WA with a slightly lower increase in activity (2.8 times). On the other hand, compound **9** showed a higher activity in lag phase ( $IC_{50}$  0.4  $\mu$ M), similar to the positive control mercaptopurine. In HeLa cells, derivatives **9**, **19**, and **54** were more active in lag phase ( $IC_{50}$  0.9, 1.2 and 0.9  $\mu$ M, respectively) as were WA and actinomycin. In addition, antitumoral activity in MCF-7 cells was time dependent. Thus, cytotoxicity of compounds **3-5**, **13**, **17**, **20**, **21**, **29**, **40**, **49**, and **52** as well as WA increased significantly (more than threefold) from 48 h to 72 h of exposure (data not shown). Moreover, we observed selectivity to a certain extent in the non-tumorigenic Vero cell line with respect to the tumor cell lines, similar as with WA, except for compound **18**, which exhibited a selectivity index (SI) of 2.5 using HeLa cells.

**Table 1**Cytotoxic activity (IC<sub>50</sub>, μM) of selected WA-analogues<sup>a</sup> in tumor cells.

Compound	HeLa		A-549		MCF-7	
	A <sup>b</sup>	B <sup>c</sup>	A <sup>b</sup>	B <sup>c</sup>	A <sup>b</sup>	B <sup>c</sup>
<b>1</b>	3.0 ± 0.1	6.3 ± 0.5	6.6 ± 0.08	10.1 ± 0.07	3.6 ± 0.02	1.3 ± 0.07
<b>3</b>	0.7 ± 0.04	1.4 ± 0.2	1.0 ± 0.1	1.4 ± 0.4	0.3 ± 0.02	0.8 ± 0.06
<b>4</b>	2.1 ± 0.6	4.9 ± 0.8	3.9 ± 0.5	4.8 ± 0.2	1.2 ± 0.4	0.9 ± 0.2
<b>5</b>	1.6 ± 0.02	1.1 ± 0.3	1.6 ± 0.5	2.1 ± 0.3	2.3 ± 0.07	1.2 ± 0.1
<b>6</b>	2.1 ± 0.1	1.1 ± 0.2	2.6 ± 0.1	4.1 ± 0.02	2.4 ± 0.3	1.1 ± 0.1
<b>7</b>	1.9 ± 0.07	1.2 ± 0.1	2.6 ± 0.03	2.2 ± 0.2	2.4 ± 0.2	1.0 ± 0.1
<b>8</b>	1.9 ± 0.3	1.6 ± 0.06	2.8 ± 0.03	1.9 ± 0.3	1.0 ± 0.3	1.0 ± 0.2
<b>9</b>	0.9 ± 0.02	2.9 ± 0.04	2.3 ± 0.3	3.7 ± 0.3	0.4 ± 0.04	1.6 ± 0.06
<b>10</b>	1.8 ± 0.2	2.9 ± 0.07	2.1 ± 0.3	3.4 ± 0.6	1.4 ± 0.09	1.5 ± 0.4
<b>11</b>	0.8 ± 0.2	1.7 ± 0.3	1.8 ± 0.1	2.1 ± 0.4	0.3 ± 0.04	0.4 ± 0.1
<b>12</b>	0.9 ± 0.09	2.4 ± 0.2	4.1 ± 0.5	4.6 ± 0.5	0.6 ± 0.1	1.2 ± 0.1
<b>14</b>	3.7 ± 0.4	4.7 ± 0.05	10.2 ± 1.0	12.2 ± 0.5	2.4 ± 0.1	3.5 ± 0.5
<b>16</b>	2.5 ± 0.1	1.1 ± 0.2	2.3 ± 0.01	3.3 ± 0.7	3.0 ± 0.4	1.0 ± 0.04
<b>17</b>	2.9 ± 0.3	3.8 ± 0.2	3.6 ± 0.1	3.8 ± 0.03	1.5 ± 0.3	1.7 ± 0.02
<b>18</b>	0.8 ± 0.01	1.6 ± 0.03	1.0 ± 0.05	1.5 ± 0.4	0.3 ± 0.1	0.7 ± 0.04
<b>19</b>	1.2 ± 0.004	3.8 ± 0.2	2.9 ± 0.2	4.2 ± 0.003	1.0 ± 0.2	2.3 ± 0.2
<b>20</b>	1.6 ± 0.2	4.2 ± 0.07	3.7 ± 0.4	4.7 ± 0.2	1.6 ± 0.1	1.0 ± 0.1
<b>21</b>	2.0 ± 0.2	3.5 ± 0.1	6.4 ± 0.02	13.7 ± 0.6	0.9 ± 0.01	2.2 ± 0.2
<b>23</b>	1.2 ± 0.3	2.1 ± 0.2	2.1 ± 0.08	1.7 ± 0.03	0.4 ± 0.06	0.6 ± 0.1
<b>24</b>	2.5 ± 0.2	2.8 ± 0.1	2.0 ± 0.3	3.6 ± 0.2	1.1 ± 0.4	1.0 ± 0.03
<b>25</b>	3.1 ± 0.4	7.9 ± 0.2	9.6 ± 0.08	18.1 ± 0.3	4.1 ± 0.1	4.8 ± 0.4
<b>26</b>	3.2 ± 0.1	3.3 ± 0.3	4.2 ± 0.1	5.3 ± 0.1	1.4 ± 0.06	1.9 ± 0.06
<b>27</b>	2.1 ± 0.01	3.8 ± 0.2	4.0 ± 0.5	4.4 ± 0.3	1.1 ± 0.2	1.7 ± 0.006
<b>28</b>	4.2 ± 0.4	7.1 ± 0.2	7.9 ± 0.09	8.3 ± 0.5	2.4 ± 0.5	2.4 ± 0.007
<b>32</b>	4.7 ± 0.02	6.8 ± 0.2	4.2 ± 0.4	8.3 ± 0.1	6.0 ± 0.2	2.3 ± 0.3
<b>33</b>	4.0 ± 0.2	1.9 ± 0.5	3.7 ± 0.2	2.3 ± 0.03	1.0 ± 0.2	1.2 ± 0.2
<b>34</b>	4.0 ± 0.2	1.9 ± 0.5	3.7 ± 0.2	2.3 ± 0.03	1.0 ± 0.2	1.2 ± 0.2
<b>35</b>	2.6 ± 0.02	1.9 ± 0.4	3.2 ± 0.02	2.3 ± 0.6	5.4 ± 0.2	1.1 ± 0.2
<b>47</b>	9.6 ± 0.4	8.4 ± 0.3	21.8 ± 0.6	9.6 ± 0.03	7.6 ± 0.1	6.9 ± 0.02
<b>54</b>	0.9 ± 0.01	3.1 ± 0.1	1.5 ± 0.02	4.0 ± 0.2	0.7 ± 0.01	1.2 ± 0.08
<b>60</b>	14.0 ± 0.1	8.0 ± 0.2	7.8 ± 0.5	8.9 ± 0.03	5.5 ± 0.2	4.8 ± 0.4
<b>64</b>	3.1 ± 0.5	3.4 ± 0.1	4.1 ± 0.08	3.8 ± 0.1	2.5 ± 0.3	3.1 ± 0.1
<b>C1<sup>d</sup></b>	1.1x 10 <sup>-3</sup> ± 10 <sup>-4</sup>	3.2x 10 <sup>-3</sup> ± 10 <sup>-4</sup>	7.2x 10 <sup>-3</sup> ± 3x10 <sup>-4</sup>	0.8x 10 <sup>-2</sup> ± 10 <sup>-2</sup>	2.4x 10 <sup>-2</sup> ± 10 <sup>-3</sup>	4.8x 10 <sup>-2</sup> ± 10 <sup>-3</sup>
<b>C2<sup>d</sup></b>	2.9 ± 0.06	4.1 ± 0.05	47.0 ± 1.9	49.4 ± 2.3	1.4 ± 0.06	5.8 ± 0.3

<sup>a</sup> WA-analogues exhibiting IC<sub>50</sub> values ranging from 0.2-9.6 μM in all tumor cell lines.<sup>b</sup> Compounds added to culture cells in lag phase of growth and incubated for 48 h.<sup>c</sup> Compounds added to culture cells in log phase of growth and incubated for 48 h.<sup>d</sup> C1 and C2: actinomycin and mercaptopurine, respectively, were used as positive controls.

### 2.2.2. Detection of apoptosis

Therapies that are designed to selectively induce apoptosis in cancer cells are currently the most promising anticancer [32]. Our group has previously reported on the apoptosis-inducing activity of withanolides isolated from *Withania aristata* and two sylyl derivatives [24] in HeLa cells. This work compares induction of apoptosis by a series of potent compounds with the structurally related, well-known, steroidal lactone WA in HeLa cervical carcinoma cells. Apoptotic nuclear morphology and oligonucleosomal, double-stranded DNA fragments (dsDNA ladder) were analyzed in HeLa cells treated with the highly potent analogues **3**, **11**, **12**, and **18** at 8, 12, 16, 24, and 32  $\mu\text{M}$  for 12 and 24 h, respectively. The extracted DNA did not exhibit the characteristic pattern of integer, 180–200 bp internucleosomal fragments in conventional gel electrophoresis at any treatment time or concentration. After treatment at 16  $\mu\text{M}$  for 12 h, a predominant smear pattern was detected in agarose gels, resembling outcomes with the previously reported withanolides [24], WA [5] and staurosporine [33], both known to induce apoptosis in many cell lines (Fig. S87 in SI).

In accordance with Meyer *et al.* [34], the apoptosis-specific 200-bp DNA ladder is overlaid by random DNA fragmentation, resulting from necrotic cell death, which may additionally appear in, e.g., imiquimod or actinomycin D treated cells. Apoptotic bodies are rapidly phagocytosed *in vivo* and, therefore, do not induce inflammation. However, they are usually not eliminated in cell cultures and finally lyses, leading to a state of secondary necrosis and a smear pattern in DNA gels. Moreover, DNA fragmentation is common to different kinds of cell death, and ICAD (caspase activated DNase inhibitor) mutant cells may even undergo apoptosis lacking the characteristic DNA cleavage. Thus, DNA fragment detection *in situ* should not be considered a specific marker for apoptosis any longer [35,36]. Characteristic nuclear morphology and double-strand DNA fragments are still being considered the hallmarks of apoptotic cell death. From a classic point of view, these two

processes occur concomitantly. Once activated, DNA fragmentation factor, 40-kDa subunit (DFF40)/caspase-activated DNase (CAD) endonuclease hydrolyzes the DNA into oligonucleosomal-size pieces, facilitating the chromatin package [36]. However, as mentioned above, the dogma that the apoptotic nuclear morphology depends on DNA fragmentation has been questioned.

In view of this rationale, we decided to check for chromatin condensation, which results in compact and smaller nuclei, the formation of apoptotic bodies or both. To this end, HeLa cells were treated with the above derivatives (**3**, **11**, **12**, and **18**) or WA at 8  $\mu$ M for 12 h, and the morphological features of apoptotic nuclei were visualized with Hoechst 33342 staining, which specifically stains for AT-rich regions in double-stranded DNA. The fluorescence photomicrographs (Fig. 2), clearly demonstrate chromatin condensation and apoptotic bodies in HeLa cells. The number of apoptotic cells upon treatment with analogues **11** and **18** was significantly higher than in untreated cells ( $p < 0.05$ ) and even higher than under WA treatment, thus resulting in approximately 28% of apoptotic nuclei compared to approximately 15% in cells treated with derivative **12**. Derivative **3** did not increase the percentage of apoptotic nuclei compared to untreated cells.

When cells are exposed to cytotoxic agents, damaged cells may suffer a block in their cell cycle at any state [37]. In this work, genomic DNA of HeLa cells was stained with propidium iodide and analyzed by flow cytometry. As shown in Fig. 3, following 12 h of treatment with derivatives **3**, **11**, **12**, and **18** at a concentration of 24  $\mu$ M, there was a general increase in the sub-G1 cell fractions. Exceptionally, treatment with compound **3** resulted in 75.2% of the cells accumulated in G1 phase without any increase in hypoploid cells, which suggests that cell death induced by this compound could derive from a distinct mechanism. It is noteworthy that the percentage of hypoploid cells induced by derivative **18** was significantly higher than even that caused by WA (22.1% vs 11.3%). The latter finding

prompted us to monitor the time course of apoptotic HeLa cell accumulation upon derivative **18** treatments. In fact, upon treatment at 16  $\mu\text{M}$  the sub-G1 cell population increased in a time-dependent manner, together with a consistently reduced G2/M population, reaching its maximum of 37.8% at 24 h. This data may suggest cell loss from the G2/M cell cycle check point through apoptosis, which agrees with a previous study on WA in melanoma cells [38].

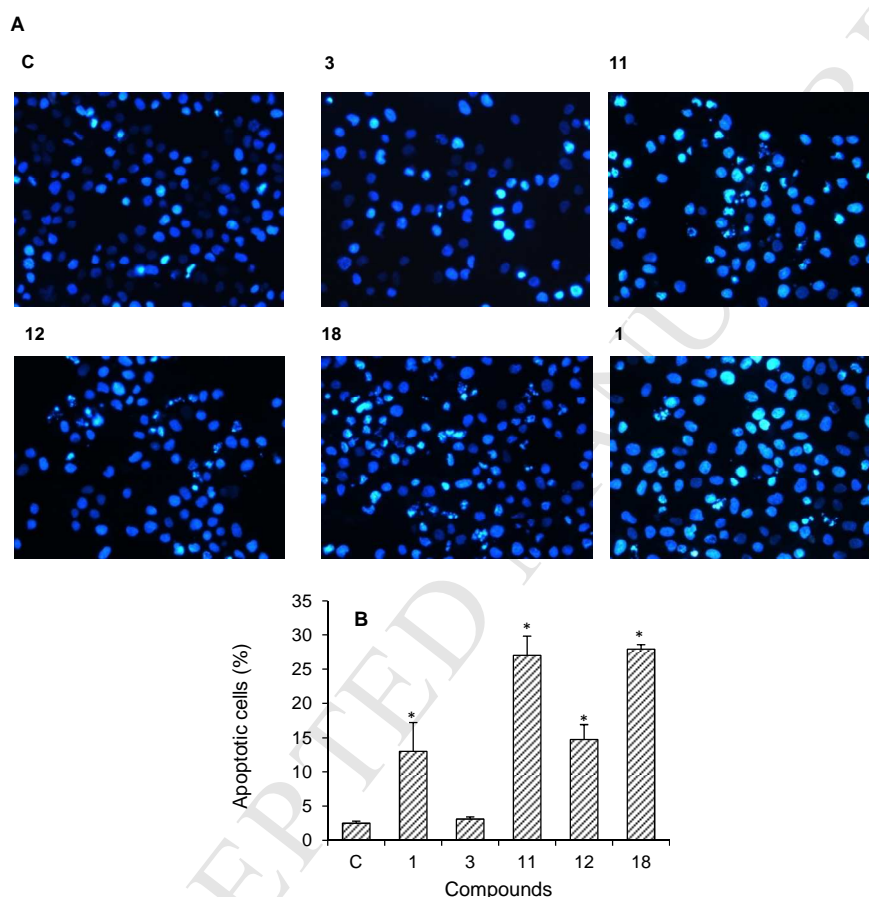


**Fig. 2.** Withanolide-induced apoptotic nuclei in HeLa cells. (A) Representative fluorescence images of apoptotic nuclei. Cells were treated with compounds **3**, **11**, **12**, **18**, and WA (**1**) at 8  $\mu\text{M}$  or with the corresponding solvent control (C) for 12 h and then stained with Hoechst 33342; amplification 20 $\times$ . (B) Percent of Hoechst-stained, apoptotic cells, calculated from a total of at least 500 per sample. Bars represent means  $\pm$  SD of three independent experiments, performed in triplicate; \* $p < 0.05$ .

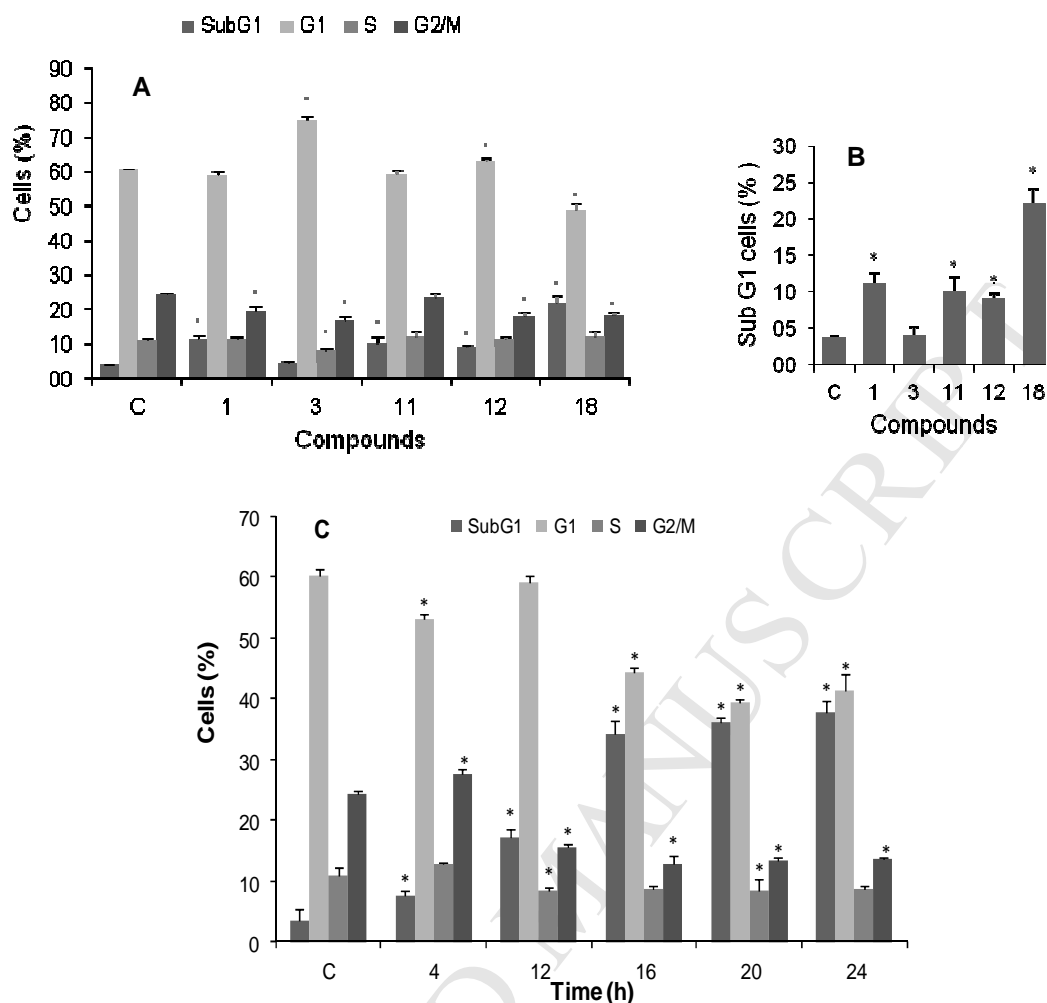


**Fig. 3.** (A) Flow cytometry analysis of HeLa cells. Cells were incubated in the absence (control) or presence of 24  $\mu\text{M}$  of the analogues **3**, **11**, **12**, **18**, or WA (**1**) for 12 h. Propidium iodide staining as described in the Experimental Section. (B) Percentages of hypoploid (Sub-G1) cells alone induced by analogues **3**, **11**, **12**, **18**, and **1** at 24  $\mu\text{M}$  for 12 h. Sub-G1 cells increased by approximately 4 to 6-fold compared to untreated controls. Derivative **18** induced a 2-fold increase compared to WA. (C) Flow cytometry analysis of HeLa cells treated with derivative **18** at 16  $\mu\text{M}$  for different time periods. Bars represent means  $\pm$  SD of at least three independent experiments, each performed in triplicates;  $p < 0.05$  (\*).

During apoptosis, early changes occur on the membrane surface, which trigger recognition and removal by macrophages and other phagocytes. Phospholipid asymmetry gets lost and results in exposure of phosphatidylserine (PS), one of the surface markers recognized by macrophages [39]. Therefore, we decided to determine the early apoptotic fraction, labeling derivative-treated HeLa cells with annexin V, a protein with a high affinity for PS, and selectively stain cells in late stage apoptosis or necrosis as their membranes get

permeable for propidium iodide (PI). As a result, early apoptotic cells (positive for PS but negative for PI) can be distinguished from late apoptotic and necrotic cells (positive for both PS and PI). Fluorescence microscopy evidenced that, in contrast to the solvent control, all analogues as well as the positive control actinomycin D, induced dose- and time- dependent PS externalization, necrosis or both in HeLa cells. Early apoptotic cells (annexin V+) were detected after treatment with compound **3** at 2  $\mu\text{M}$  for 30 min, whereas 4  $\mu\text{M}$  led to early and late stage apoptosis (annexin V+/PI+). Exclusively necrotic (PI+) cells were observed when HeLa cells were exposed to 4  $\mu\text{M}$  of the same derivative for 4 h and to 8  $\mu\text{M}$  for 30 minutes (data not shown). Similarly, early and late stage apoptosis were observed after treatment with compound **18** at 4 and 8  $\mu\text{M}$  for 1 h, respectively (Fig. 4). Higher concentrations of derivatives **11** (12  $\mu\text{M}$ ) and **12** (10  $\mu\text{M}$ ) and a longer incubation period (4 h) were required to lead to apoptosis. Likewise, WA required a maximum exposure time of 4 h to induce detectable PS externalization.

Altogether, these data strongly suggest that the analyzed analogues induce apoptosis in HeLa cells in a dose- and time-dependent manner. However, chromatin condensation is often found in necrotic cells as well, and the presence of apoptotic bodies does not ensure that apoptosis is the mechanism of the cell death [40]. Moreover, as shown above, apoptosis and necrosis can occur simultaneously in tissues or cell cultures exposed to a single stimulus. The intensity of the initial insult frequently determines over the prevalence of either apoptosis or necrosis. Hence, the evaluation of apoptosis activating or executing proteins may help characterize the ongoing cell death. Caspases are crucial mediators of apoptosis. Specifically, the death effector protease caspase-3 is commonly activated, catalyzing the specific cleavage of various, cellular key proteins. Its role in programmed cell death has been shown to be remarkably specific depending on the type of tissue, cell, or death stimulus. The activation of caspase-3 leads to characteristic changes in cell morphology and certain biochemical events

associated with the execution and completion of apoptosis [41] and terminates in chromosomal DNA degradation [40].

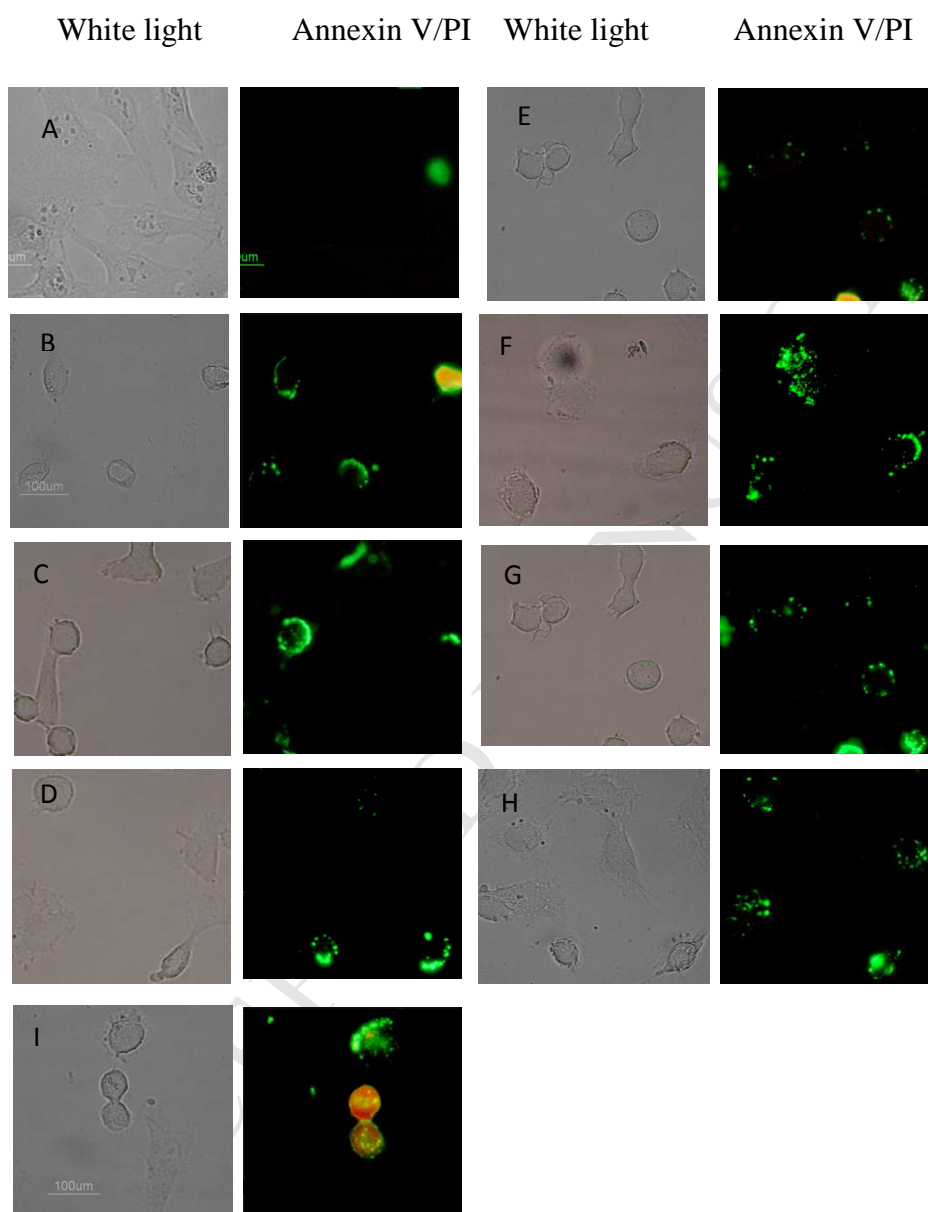


**Fig. 4.** Fluorescence photomicrographs from withanolide-treated, early apoptotic HeLa cells, characterized by external, phosphatidylserine (PS) membrane expression; amplification 40 $\times$ . (A) DMSO solvent control. (B) Actinomycin D at 1  $\mu$ M for 1 h. (C) WA at 2  $\mu$ M for 4 h. (D–E) Analogue **3** at 2 and 4  $\mu$ M for 30 min. (F–G) Analogues **11** and **12** at 12 and 10  $\mu$ M, respectively for 4 h. (H–I) Analogue **18** at 4 and 8  $\mu$ M for 1 h.

To characterize the ongoing cell death in analogue-treated HeLa cells, possible caspase-3 activation was determined, extending this study to additional analogues with a notable antiproliferative potential ( $IC_{50}$  values ranging from 1.1 to 1.9  $\mu\text{M}$  in HeLa cells), namely compounds **5-8**, **16** and **35**. On the whole, the studied analogues induced caspase-3 activation, assessed by colorimetric technique, in HeLa cells in a dose-dependent manner at concentrations above 8  $\mu\text{M}$ , while enzyme activity at 4  $\mu\text{M}$  did not differ from that in untreated cells ( $0.23 \text{ nmolpNA/min/ml} \pm 0.063$ , Table 2). Particularly, derivatives **5-8**, **11**, **16**, and **18** increased enzyme activity, compared to WA, significantly ( $p < 0.05$ ) from 12  $\mu\text{M}$  upward. Of note, derivative **6** induced a higher caspase-3 activity at 16  $\mu\text{M}$  than the positive control staurosporine at 2  $\mu\text{M}$  for 4 h ( $1.92 \text{ nmolpNA/min/ml} \pm 0.13$ ). However, caspase-3 activity declined ( $> 50\%$ ) upon treatment with compounds **3** and **35** at 32  $\mu\text{M}$  (4 h). This phenomenon was probably caused by the associated loss of cellular integrity and adhesion observed by light microscopy (data not shown).

To determine whether caspase-3 activity could further increase with time, HeLa cells were treated with the analogues (except for **3** and **35**) at a fixed concentration of 24  $\mu\text{M}$  for 8 h. In fact, caspase-3 activity further augmented significantly ( $p < 0.05$ ) within 8 h, mainly upon exposure to derivative **18** ( $1.7\text{-}2 \text{ nmolpNA/min/ml}$ ) resembling the effect of WA ( $0.6\text{-}1.9 \text{ nmolpNA/min/ml}$ ) (Fig. 5). By contrast, treatment with the other derivatives at 32  $\mu\text{M}$  for 8 h produced a significant decrease in caspase-3 activity, associated with drastic cell damage.

**Table 2**

Caspase-3 activity<sup>a</sup> in HeLa cells treated with selected WA-analogues at different concentrations for 4 h.

Compound	Caspase-3 activity (nmol pNA/min/mL)				
	8 $\mu$ M	12 $\mu$ M	16 $\mu$ M	24 $\mu$ M	32 $\mu$ M
<b>1</b>	0.35 $\pm$ 0.01	0.41 $\pm$ 0.01	0.47 $\pm$ 0.05	0.55 $\pm$ 0.02	1.12 $\pm$ 0.11
<b>3</b>	0.33 $\pm$ 0.08	0.42 $\pm$ 0.01	0.50 $\pm$ 0.06	1.06 $\pm$ 0.12*	0.68 $\pm$ 0.12
<b>5</b>	0.52 $\pm$ 0.15*	0.52 $\pm$ 0.02*	1.02 $\pm$ 0.05*	1.90 $\pm$ 0.13*	1.67 $\pm$ 0.04*
<b>6</b>	0.58 $\pm$ 0.1*	1.10 $\pm$ 0.02*	2.30 $\pm$ 0.02*	1.6 $\pm$ 0.02*	1.70 $\pm$ 0.02*
<b>7</b>	0.54 $\pm$ 0.1*	0.72 $\pm$ 0.1*	1.22 $\pm$ 0.09*	1.24 $\pm$ 0.07*	1.33 $\pm$ 0.01*
<b>8</b>	0.15 $\pm$ 0.03	0.61 $\pm$ 0.07*	0.93 $\pm$ 0.09*	0.88 $\pm$ 0.09*	1.70 $\pm$ 0.1*
<b>11</b>	0.26 $\pm$ 0.06	0.61 $\pm$ 0.01*	0.78 $\pm$ 0.04*	1.04 $\pm$ 0.05*	0.93 $\pm$ 0.08
<b>12</b>	0.26 $\pm$ 0.003	0.25 $\pm$ 0.02	0.28 $\pm$ 0.03	0.54 $\pm$ 0.04*	0.63 $\pm$ 0.02
<b>16</b>	0.44 $\pm$ 0.14	0.68 $\pm$ 0.04*	0.62 $\pm$ 0.05*	1.01 $\pm$ 0.1*	1.63 $\pm$ 0.05*
<b>18</b>	0.32 $\pm$ 0.14	0.52 $\pm$ 0.04*	0.67 $\pm$ 0.05*	1.16 $\pm$ 0.1*	0.85 $\pm$ 0.05
<b>35</b>	0.65 $\pm$ 0.08*	0.40 $\pm$ 0.11	0.67 $\pm$ 0.06*	1.05 $\pm$ 0.03*	0.61 $\pm$ 0.02

<sup>a</sup> Values represent means  $\pm$  SD of three independent experiments, each performed in triplicate. \*Significant increase difference compared to treatment with WA (**1**),  $p < 0.05$ .

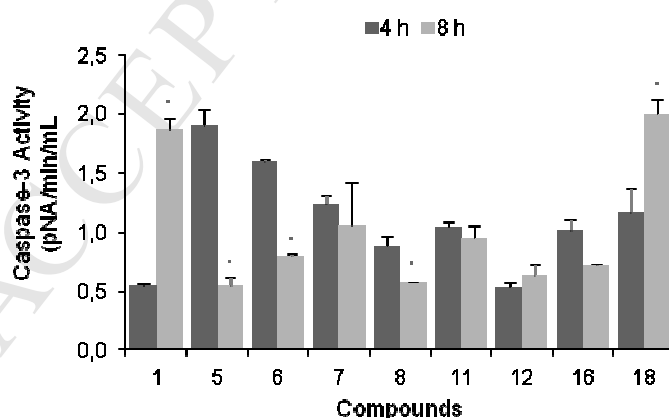


**Fig. 5.** Caspase-3 activity in HeLa cells treated with compounds **1** (WA), **5-8**, **11**, **12**, **16**, and **18** at 24  $\mu$ M for 4 h and 8 h, respectively. Values represent means  $\pm$  SD of three independent experiments, each performed in triplicate; significance of variation between treatments for 4 h and 8 h,  $p < 0.05$  (\*).

### 2.3. Structure-activity relationship analysis

Despite the well-recognized antitumor properties of WA, limited attempts have been made to decipher SAR studies [18,22,28,42-45]. The previous reported SAR studies agree in that the  $\alpha,\beta$ -unsaturated ketone on ring A, the  $5\beta,6\beta$ -epoxide in ring B and the C9 side-chain with an  $\alpha,\beta$ -unsaturated  $\delta$ -lactone group, are antitumor structural features requirements. Therefore, a detailed investigation of the importance of functionalities is highly desirable.

In this work, the influence of the substitution pattern on the cytotoxic activity of the compounds under study (**1-64**) was carried out taking into consideration the  $IC_{50}$  values against the cell lines assayed (Tables S83-S86 in SI). WA and the known cytotoxic activity of compounds **2**, **52**, **54**, and **56**, previously reported by our group [23,24] have been included to broaden the SAR analysis, and for comparative purposes. The trends of the SAR study from this series of withanolides were as follows (see Fig. 6).

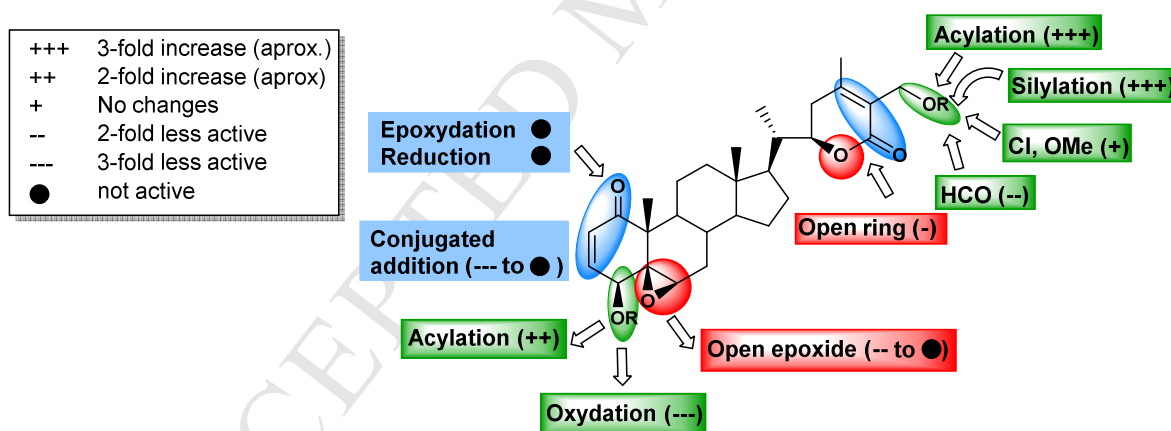


**Fig. 6.** Summary of the structure-cytotoxic activity relationship in WA-analogues.

A) First, we analyzed the role of the hydroxyl groups at C-4 and C-27 on the activity. Thus, comparison of the activity of the two groups of ester analogues, the 27-ester (**2**, **4**, **5**, **7**, **9**, **11**, **14**, **16**, and **18-21**) and the 4,27-diester (**3**, **6**, **8**, **10**, **12**, **13**, **15**, **17**, **22**, and **23**) withanolides (Scheme 1, Table S83 in SI), showed a clear increase of activity with respect to

the non-acylated WA. Moreover, the presence of a second ester group at C-4 led to a marginal (e. g. **5** > **6**, **11** > **12**) or null (e. g. **7**  $\approx$  **8**) differences between both series, except for the diacetylated **3**. In addition, when the ester possesses an alkyl chain (**2-14**), the optimum number of carbons seems to be four or five (e.g. **7** and **12** vs **13**). Furthermore, an ester with a non-substituted aromatic ring led to one of the most promising antiproliferative analogues (**18**, 27-Bz), suggesting additional  $\pi$ - $\pi$  interactions with the binding site could be involved. However, the presence of an electron-withdrawing (**19**, 27-*p*-BrBz) or electron-donor (**20**, *o*-MABz) substituent at any position of the phenyl ring does not exert a clear influence on the activity when compared with **18** (27-Bz). Also the replacement of the benzyl group in **18** with bioisosteres, such as furyl or naphthyl motif (**16** and **21**, respectively) does not produce significant changes in the activity. These results are in line with our preliminary reports [23] on the role of ester moieties to increase activity.

B) The effect of modifications on the 27-hydroxymethylene and on the 4-hydroxy group was investigated by chloration and methylation of WA, which yielded analogues **24** and **25**, and **26** and **27**, respectively (Scheme 2). Although active, these analogues showed marginal or null increase of activity compared to WA (Table S84 in SI). Analogue **28**, bearing an opened  $\delta$ -lactone ring, has a slightly lesser effect on the cells.

C) Considering it has been reported [24] that the presence of a carbonyl group at C-4 might increase selectivity, analogues **29-35** were prepared by two different conditions of oxidation (Schemes 2 and 3, Table S84 in SI). Comparison of IC<sub>50</sub> values displayed by WA with those of **29** (4-OH, 27-aldehyde) and **30** (4-oxo, 27-aldehyde) indicated that the presence of an H-bond acceptor substituent at C-27 or C-27/C-4 produce an over 2 or 3-fold decrease in the activity, respectively. This is in agreement with results obtained for compounds **31-35**, the 4-oxo-analogues of compounds **2**, **5**, **7**, **11**, and **18**, respectively. These

results indicated that neither the activity nor the selectivity was improved when the 4-OH was switched for a carbonyl group.

D) Previous SAR studies correlate the biological activity of withanolides with the presence of Michael acceptors in the form of  $\alpha,\beta$ -unsaturated carbonyl systems in their structure [18,19]. In order to confirm this, analogues **36-49** (Schemes 4 and 5) were prepared by reduction or conjugated nucleophilic addition reactions. All derivatives were less active than the lead (Table S85 in SI). Thus, the reduction of the 1-keto group and/or the  $\Delta^2$  double bond of WA yielded analogues **40** and **38**, respectively, which were found to be inactive as well as **41** and **42**, the hydrogenated derivatives of **40**. Likewise, the 2,3-epoxy-analogues, **36** and **37**, were also found to be inactive (Scheme 5). Adducts **43-49**, prepared by conjugated nucleophilic addition of water, alcohols or amines, displayed very low activity, except **47** and **48**, which exhibited moderate activity against the three cell lines.

E) To explore the relevance of the epoxide moiety into the molecular scaffold of WA, compounds **50-52**, **55** and **56** were prepared by  $5\beta,6\beta$ -epoxy ring-opening under different mild reaction conditions (Scheme 6). All derivatives were less active than the parent compound (e. g. **56** and **55** vs **1** and **54**, respectively, Table S86 in SI), in concordance with previous findings [21]. Thus, epoxy ring-opening along with introduction of a substituent at C-3 (**50** and **51**) led to a decrease in the activity. Compound **52** obtained by ring-A rearrangement was also inactive (Scheme 6). Two further modifications were performed on these ring-opening analogues in order to evaluate the importance of the 27-hydroxylmethylene group. First, when a silyl ether functionality (TBDMS) was introduced at C-27 position of **56** to obtain compound **64** (Scheme 6, Table S86 in SI), the activity enhanced 3 to 4-fold, in accordance with previous reports [24], although more analogues are required to draw firm conclusions. Second, a series of chloroester derivatives (**57-63**) were

prepared from the chlorohydrin **56**. Interestingly, analogues **62** and **63** (mono and di-*p*-MeOBz esters) showed selectivity on MCF-7 cell line, exhibiting a 2-fold increase in activity.

This SAR study (Fig. 6), in accordance with previous works, confirms that an  $\alpha,\beta$ -unsaturated ketone on ring A, a  $5\beta,6\beta$ -epoxide in ring B and a C9 side-chain with an  $\alpha,\beta$ -unsaturated  $\delta$ -lactone group in the molecular scaffold of withanolides are essential for antiproliferative activity. In addition, this study clearly demonstrates that acylation enhances the cytotoxicity.

### 3. Conclusions

In summary, we have successfully designed and synthesized a series of potent apoptotic inducers by a molecular fine tuning of the WA framework. The evaluation of withaferin A-analogue library for their anticancer potential in three human cancer cell lines, HeLa, A-549, and MCF-7, and the Vero non-tumoral cell line, led to thirteen analogues with an improved profile compared to the lead compound. A detailed SAR analysis confirms that an  $\alpha,\beta$ -unsaturated ketone on ring A, a  $5\beta,6\beta$ -epoxide in ring B and a C9 side-chain with an  $\alpha,\beta$ -unsaturated  $\delta$ -lactone group in the WA framework are antitumor structural requirements. In addition, the SAR trends revealed that acylation enhances cytotoxicity, presumably by increasing affinity and/or cell membrane permeability. Taken together, our results demonstrate that derivatives studied in this work induce apoptosis in HeLa cells in a dose- and time-dependent manner, evidenced by chromatin condensation, PS externalization, and caspase-3 activation. WA-27-benzyl analogue (**18**) showed a potent capacity to induce apoptosis in HeLa cells with concomitant cell cycle arrests in G2/M, surpassing that of WA. Therefore, analogue **18** could be considered as promising candidates in anticancer drug development that deserve further investigation.

## 4. Experimental

### 4.1. General

Optical rotations were measured on a Perkin Elmer 241 automatic polarimeter, in  $\text{CHCl}_3$  at 25 °C, the  $[\alpha]_D$  values are given in units of  $10^{-1} \text{ deg cm}^2 \text{ g}^{-1}$ . UV spectra were obtained on a JASCO V-560 in absolute EtOH, and IR (film) spectra on a Bruker IFS 55 spectrophotometer.  $^1\text{H}$  (400, 500 or 600 MHz) and  $^{13}\text{C}$  (100, 125 or 150 MHz) NMR spectra were recorded on a Bruker Avance 400 spectrometer; chemical shifts are given in ppm and coupling constants in Hz. Solutions were typically prepared in either  $\text{CDCl}_3$  or  $\text{CD}_3\text{OD}$  with chemical shifts referenced to deuterated solvent as an internal standard; DEPT COSY, ROESY (spin lock field 2500 Hz), HSQC, and HMBC (optimized for  $J = 7.7 \text{ Hz}$ ) experiments were carried out with the pulse sequences given by Bruker. EIMS and HREIMS were measured on a Micromass Autospec spectrometer, and ESIMS and HRESIMS (positive mode) were measured on a LCT Premier XE Micromass Autospec spectrometer. Silica gel 60 for column chromatography (particle size 15-40 and 63-200  $\mu\text{m}$ ), Polygram Sil G/UV<sub>254</sub> used for analytical and preparative TLC, and HPTLC-Platten Nano-Sil 20 UV<sub>254</sub> were purchased from Macherey-Nagel. Reactions were monitored by TLC, the spots were visualized by UV light and heating silica gel plates sprayed with  $\text{H}_2\text{O}-\text{H}_2\text{SO}_4-\text{AcOH}$  (1:4:20). Varian high-performance liquid chromatography (HPLC) equipment consisted of a ProStar 210 solvent delivery module, ProStar 335 photodiode array detector, using an analytical Pursuit C18 column (2.0 x 100 mm, 3  $\mu\text{m}$ ) with a flow rate of 0.3 mL/min, and mixtures of acetonitrile- $\text{H}_2\text{O}$  as eluent. The degree of purity of the compounds was over 95% as indicated by the appearance of a single peak using HPLC. Unless otherwise noted, solvents and reagents were obtained from commercial suppliers and used without further purification. Anhydrous THF and  $\text{CH}_2\text{Cl}_2$  were distilled from sodium/ benzophenone and calcium hydride ketyl under

nitrogen, respectively. All solvents used were analytical grade from Panreac, and the reagents were purchased from Sigma Aldrich. Withaferin A (WA, **1**), used as starting material, was isolated from the leaves of *W. aristata* as previously described [24].

#### 4.2. Plant material

Leaves of *Withania aristata* (Ait.) Pauq. (Solanaceae) were collected in Icod de los Vinos, Tenerife, Canary Islands (Spain), in May 2010. A voucher specimen (TFC 48.068) is deposited in the Herbarium of the Department of Botany, University of La Laguna, Tenerife, and identified by Leticia Rodríguez-Navarro.

#### 4.3. Biological assays

##### 4.3.1. Cell culture

HeLa (human cervix carcinoma), A-549 (human lung carcinoma), MCF-7 (human breast adenocarcinoma), and Vero (African green monkey kidney) cell lines from ATCC-LGC (American Type Culture Collection) were all grown in Dulbecco's modified Eagle's medium (DMEM) with 4.5 g/L glucose (Sigma-Aldrich), supplemented with 10% fetal bovine serum (Gibco), 1% of a penicillin-streptomycin mixture (10,000 UI/mL and 10 mg/mL, respectively), and 200 mM L-glutamine. Cells were maintained at 37 °C in 5% CO<sub>2</sub> and 98% humidity.

##### 4.3.2. Cell viability assay

Viable cells were assessed using the colorimetric MTT [3-(4,5-dimethylthiazol-2-yl)-2,5-diphenyl tetrazolium bromide] reduction assay [46]. Cell suspensions ( $2 \times 10^4$ /100  $\mu$ L/well) were either incubated for 48 h with the compounds at different concentrations pre-

dissolved in dimethyl sulfoxide (DMSO), 24 h past seeding in 96-well plates (Iwaki, London, UK) (log-phase incubation) or seeded together with the compounds and incubated for either 48 h or 72 h (lag-phase incubation). Therefore, 20  $\mu$ L/well of the MTT solution (5 mg/mL in phosphate buffered saline, PBS) was added, and plates incubated for 3 h at 37 °C. Subsequently, the medium was aspirated and replaced with 150  $\mu$ L/well of DMSO to dissolve the formazan crystals. Absorbance was measured in a microplate reader (Tecan Group Ltd., Männedorf, Switzerland) at a wavelength of 550 nm. Solvent control cultures were considered 100%, and viable treated cells (percent) were plotted against compound concentrations. The 50% cell viability value ( $IC_{50}$ ) was calculated from the curve. Each experiment was performed at least three times in triplicates. Data are given in arithmetic means  $\pm$  SD. Selectivity ratios were defined as the  $IC_{50}$  value for the corresponding tumor cell line divided by the  $IC_{50}$  value for the Vero cell line.

#### 4.3.3. Detection of DNA fragmentation

HeLa cells were incubated in 24-well plates with varying concentrations of each compound or the respective volume of DMSO (solvent control) for various time periods. Cells treated with staurosporine at a concentration of 2  $\mu$ M were used as a positive control. Following incubation, adherent and floating cells were collected, centrifuged at 500 g for 10 min, and washed twice with cold PBS. Then, DNA was extracted using Gen Elute™ Mammalian genomic DNA kit according to the manufacturer's protocol (Sigma-Aldrich). DNA samples were analyzed by agarose gel electrophoresis in 1.8% agarose, followed by ethidium bromide (Sigma-Aldrich) staining and visualization with UV.

#### 4.3.4. Detection of chromatin condensation

To identify apoptotic, nuclear changes (such as chromatin condensation), HeLa cells in 6-well plates were treated with the compounds at 8  $\mu$ M for 12 h. Thereafter, adherent and floating cells were collected, centrifuged at 500 g for 10 min, and washed twice with PBS, fixed in 3% paraformaldehyde (in PBS), and stained with 10  $\mu$ L Hoechst 33342 (16  $\mu$ g/mL) for 15 min. The (polylysine-coated) slides with the cells were inspected for nuclear morphological alterations and apoptotic bodies by fluorescence microscopy (*Leica*, DM 4000 B) and microphotographs taken by a coupled digital camera (Nikon DXM1200F). To quantify data, an area containing at least 500 cells was evaluated on each slide. Only cells the chromatin of which had split into more than three fragments were rated as. Data were expressed as the percent of total cell numbers.

#### 4.3.5. Flow cytometry analysis

1–2 $\times$ 10<sup>6</sup> HeLa cells per 6-well were exposed to compounds at 24  $\mu$ M for 12 h. Thereafter, adherent and floating cells were collected, centrifuged at 500g for 10 min, washed twice with ice-cold PBS, fixed and permeabilized with ice-cold ethanol at 70%, and kept at -20 °C overnight. Then, cells were centrifuged as above at 4 °C, washed twice with PBS and incubated with 100  $\mu$ g/mL RNase A, together with 50  $\mu$ g/mL propidium iodide (PI), under light protection, at room temperature for 1 h. At least 1 $\times$ 10<sup>4</sup> cells per sample were analyzed in an Epics XL-MCL flow cytometer (Beckman Coulter, CA).

#### 4.3.6. Caspase-3 activity assay

Caspase-3 activity was determined using a colorimetric assay (Molecular Probes/Invitrogen, Carlsbad, CA) according to the manufacturer's protocol. HeLa cells (1 $\times$ 10<sup>6</sup>/6-well) were incubated for the indicated time periods in the presence or absence of

different concentrations of the compounds (4, 8, 12, 16, 24, and 32  $\mu\text{M}$ ) for 4 h or together with 2  $\mu\text{M}$  of staurosporine, used as a positive control. Adhered and floating cells were then harvested, centrifuged at 300 g for 5 min, and washed twice in cold PBS. The pellets were lysed at 4 °C in 100  $\mu\text{L}$  of lysis buffer for 10 min. Lysates were centrifuged at 16,000 g for 2 min, and total protein in supernatants was determined by Bradford assay (Bio-Rad, Hercules, CA). Caspase-3 activity assays were performed in 96-well plates by incubating 50  $\mu\text{g}$  of protein in 50  $\mu\text{L}$  of reaction buffer and 5  $\mu\text{L}$  of the 4 mM chromogenic substrate, Ac-DEVD-pNA (acetyl-Asp-Glu-Val-Asp *p*-nitroanilide), at 37 °C for 2 h. Absorbance of released *p*-nitroaniline was measured at 405 nm (Tecan Group Ltd., Männedorf, Switzerland) and activity of caspase-3 evaluated by calculating OD (optical density) ratios of treated/untreated samples. Experiments were performed in triplicates.

#### 4.3.7. Phosphatidylserine labelling

$1.6 \times 10^5$  HeLa cells each were grown on coverslips in 24-wells and treated with 2–16  $\mu\text{M}$  of the corresponding compound for 30 min, 1, 2, and 4 h or with the equivalent volume of DMSO (solvent control) or actinomycin D at 1  $\mu\text{M}$  (positive control) for different time periods. Phosphatidylserine externalization and cell permeability were assessed by Annexin V/PI double staining (Vybrant® Apoptosis Assay Kit #2, Invitrogen, Molecular Probes™) according to the manufacturer's instructions. Apoptotic cells were recognized by fluorescence microscopy (Leica, DM 4000 B) and microphotographs taken with a coupled digital camera (Nikon DXM1200F). Annexin V<sup>+</sup>/PI<sup>-</sup> cells were considered early apoptotic, whereas Annexin V<sup>+</sup>/PI<sup>+</sup> cells were rated as late apoptotic/necrotic.

4.3.8. *Statistical analysis.* All results were expressed as means  $\pm$  SD. Significant differences between groups were determined using unpaired Student's *t*-test. Significance was set at  $p < 0.05$ .

## Acknowledgments

This study was supported by the Fundación CajaCanarias SALUCAN03 project, and SAF2015-65113-C2-1-R and AGL2015-63740-C2-2-R MINECO, Spain projects and by FEDER funds from the EU.

## Appendix A. Supplementary material

Supplementary material associated with this article can be found, in the online version.

## References

- [1] Cancer: Fact Sheet no. 297; World Health Organization: Geneva, 2015; <http://www.who.int/mediacentre/factsheets/fs297/en/> (accessed April 15, 2017).
- [2] W. Hu, J.J. Kavanagh, *Lancet. Oncol.* 4 (2003) 721-729.
- [3] L-X. Chen, H. He, F. Qiu, *Nat. Prod. Rep.* 28 (2011) 705-740.
- [4] K. Rishu, N. Kaushik, *Phytochem. Rev.* (2017) d.o.i. 10.1007/s11101-017-9504-6.
- [5] W. Vanden Berghe, L. Sabbe, M. Kaileh, G. Haegeman, K. Heyninck, *Biochem. Pharmacol.* 84 (2012) 1282-1291.
- [6] A. R. Vyas, S. V. Singh, *AAPS* 16 (2014) 1-10.
- [7] Ch. S. Chirumamilla, C. Perez-Novo, O.X. Van, W.V. Berghe, *Proc. Nutr. Soc.* (2017) 1-10.

- [8] M.L. Antony, J. Lee, E.-R. Hahm, S.-H. Kim, A.I. Marcus, V. Kumari, X. Ji, Z. Yang, C.L. Vowell, P. Wipf, G.T. Uechi, N.A. Yates, G. Romero, S.N. Sarkar, S.V. Singh, J. Biol. Chem. 289 (2014) 1852-1865.
- [9] E.-R. Hahm, M.B. Moura, E.E. Kelley, B. Van Houten, S. Shiva, S.V. Singh, PloS One 6 (2011) e23354.
- [10] L. Piao, C. Zhao, W. Lu, X. Cheng, W. Shi, L. Li, Mol. Immunol. 81 (2017) 92-101.
- [11] R. Munagala, H. Kausar, C. Munjal, R.C. Gupta, Carcinogenesis 32 (2011) 1697-1705.
- [12] Y. Nishikawa, D. Okuzaki, K. Fukushima, S. Mukai, S. Ohno, Y. Ozaki, N. Yabuta, H. Nojima, PloS One 10 (2015) e0134137.
- [13] B.Y. Choi, B.-W. Kim, J. Cancer Prev. 20 (2015) 185-192.
- [14] T.P. Das, S. Suman, H. Alatassi, M.K. Ankem, C. Damodaran, Cell Death and Disease 7 (2016) e2111.
- [15] A. Nagalingam, P. Kuppusamy, S.V. Singh, D. Sharma, N.K. Saxena, Cancer Res. 74 (2014) 2617-2629.
- [16] Z.-G. Cui, J.-L. Piao, M.U.R. Rehman, R. Ogawa, P. Li, Q.-L. Zhao, T. Kondo, H. Inadera, Eur. J. Pharmacol. 723 (2014) 99-107.
- [17] J. Lee, E.-R. Hahm, A. I. Marcus, S.V. Singh, Mol. Carcinogenesis 54 (2015) 417-429.
- [18] S. K. Yousuf, R. Majeed, M. Ahmad, P.L. Sangwan, B. Purnima, A.K. Saxsena, K.A. Suri, D. Mukherjee, S.C. Taneja, Steroids 76 (2011) 1213-1222.
- [19] E.M. Kithsiri Wijeratne, Y.-M. Xu, R. Scherz-Shouval, M.T. Marron, D.D. Rocha, M.X. Liu, L.V. Costa-Lotufo, S. Santagata, S. Lindquist, L. Whitesell, A.A.L. Gunatilaka, J. Med. Chem. 57 (2014) 2851-2863.
- [20] S. Tao, J. Tillotson, E.M.K. Wijeratne, Y. Xu, M. Kang, T. Wu, E.C. Lau, C. Mesa, D.J. Mason, R.V. Brown, J.J. La Clair, A.A.L. Gunatilaka, D.D. Zhang, E. Chapman. ACS Chem. Biol. 10 (2015) 1916-1924.

- [21] Y.P. Bharitkar, S. Kanhar, N. Suneel, S.K. Mondal, A. Hazra, N.B. Mondal, *Mol. Divers.* 19 (2015) 251-261.
- [22] T. Tahara, U. Streit, H.E. Pelish, m.D. Shair, *Org. Let.* 19 (2017) 1538-1541.
- [23] G.G. LLanos, L.M. Araujo, I.A. Jiménez, L.M. Moujir, J.T. Vázquez, I.L. Bazzocchi, *Steroids* 75 (2010) 974-981.
- [24] G.G. LLanos, L.M. Araujo, I.A. Jiménez, L.M. Moujir, I.L. Bazzocchi, *Eur. J. Med. Chem.* 54 (2012) 499-511.
- [25] L. Gambhir, R. Checker, D. Sharma, M. Thoh, A. Patil, M. Degani, V. Gota, S.K. Sandur, *Toxicol. Appl. Pharmacol.* 289 (2015) 297-312.
- [26] A.L. Gemal, J.L. Luche, *J. Am. Chem. Soc.* 103 (1981) 5454-5459.
- [27] D. Lavie, Y. Kashman, E. Glotter, N. Danieli, *J. Chem. Soc. C* (1966) 1757-1764.
- [28] B. Jayaprakasam, Y. Zhang, N.P. Seeram, M.G. Nair, *Life Sciences* 74 (2003) 125-132.
- [29] S.W. Pelletier, G. Gebeyehu, J. Nowacki, N.V. Mody, *Heterocycles* 15 (1981) 317-320.
- [30] H. Zhang, A.K. Samadi, R.J. Gallagher, J.J. Araya, X. Tong, V.W. Day, M.S. Cohen, K. Kindscher, R. Gollapudi, B.N. Timmermann, *J. Nat. Prod.* 74 (2011) 2532-2544.
- [31] G.A. González, J.L. Breton, J.M. Trujillo, *An. Quím.* 70 (1974) 69-73.
- [32] S.W. Fesik, *Nature Rev. Cancer* 5 (2005) 876-885.
- [33] D. Tang, J.M. Lahti, V.J.J. Kidd, *Biol. Chem.* 275 (2000) 9303-9307.
- [34] T. Meyer, I. Nindl, T. Schmook, C. Ulrich, W. Sterry, E. Stockfleth, *J. Brit. Dermatol.* 149 (2003) 9-13.
- [35] S. Nagata, *Exp. Cell Res.* 256 (2000) 12-18.
- [36] V.I. Guimaraes, E. Gil-Giñon, M. Sánchez-Osuna, E. Casanelles, M. García Belinchon, J.X. Comella, V.J. J. Yuste, *Biol. Chem.* 288 (2013) 9200-9215.
- [37] F. McLaughlin, P. Finn, N.B. La Thangue, *Drug Discov. Today* 8 (2003) 793-802.

- [38] E. Mayola, C. Gallerne, D.D. Esposti, C. Martel, A. Pervaiz, L. Larue, B. Debuire, A. Lemoine, C. Brenner, C. Lemaire, *Apoptosis* 16 (2011) 1014-1027.
- [39] V.A. Fadok, A. Cathelineau, D.L. Daleke, P.M. Henson, D.L. Bratton, *J. Biol. Chem.* 276 (2001) 1071-1077.
- [40] S. Elmore, *Toxicol. Pathol.* 35 (2007) 495-516.
- [41] A.G. Porter, R.K. Jänicke, *Cell Death Differ.* 6 (1999) 99-104.
- [42] H.-Ch. Wang, Y.-L. Tsai, Y.-Ch. Wu, F.-R. Chang, M.-H. Liu, W.-Y. Chen, Ch.-Ch. Wu, *PLoS One* 7 (2012) e37764.
- [43] H. Zhang, A.K. Samadi, M.S. Cohen, B.N. Timmermann, *Pure Appl. Chem.* 84 (2012) 1353-1367.
- [44] D. Nakano, K. Ishitsuka, H. Katsuya, N. Kunami, R. Nogami, Y. Yoshimura, M. Matsuda, M. Kamikawa, R. Tsuchihashi, M. Okawa, T. Ikeda, T. Nohara, K. Tamura, J. Kinjo, *J. Nat. Med.* 67 (2013) 415–420.
- [45] M. Gu, Y. Yu, G.M.K.B. Gunaherath, A.A.L. Gunatilaka, D. Li, D. Sun, *Invest. New Drugs* 32 (2014) 68-74.
- [46] T. Mosmann, *J. Immunol. Methods* 65 (1983) 55-63.

**Research highlights**

A withaferin A-based library of 63 compounds was prepared.

Fifteen analogues displayed higher antiproliferative effects than withaferin A.

Hoechst, Annexin V/PI and caspase-3 studies revealed that compounds induce apoptosis.

Structure-activity relationships revealed that acylation enhances cytotoxicity

WA-27-benzyl analogue, a promising apoptotic inducer drug candidate.